

Electrical Conductivity of Lignocellulose Composites Loaded with Electrodeposited Copper Powders

M.M. Pavlović^{1,*}, V. Čosović¹, M.G. Pavlović², N. Talijan¹, V. Bojanić³

¹University of Belgrade, ICTM-CMM, 11000 Belgrade, Njegoševa 12, Serbia

²University of Belgrade, ICTM-CEH, 11000 Belgrade, Njegoševa 12, Serbia

³University of Banja Luka, Agrifaculty, Banja Luka, Republic of Srpska

*E-mail: mpavlovic@tmf.bg.ac.rs

Received: 11 July 2011 / *Accepted:* 15 August 2011 / *Published:* 1 September 2011

Composites based on polymers with conductive fillers have been gaining more and more significant roles in a variety of technological domains and are in the research focus of numerous studies as a part of growing research trend. Natural polymers based on renewable materials with addition of chosen materials can be directly used as contemporary materials by electrochemical methods. This article is concerned with the preparation characterization of the basic components: electrodeposited copper powder and lignocellulose as well as composite materials prepared by the compression molding of lignocellulose and galvanostatically obtained copper powder mixtures. Analysis of the most significant properties of individual components and prepared composites included quantitative structural analysis, morphological analysis, determination of density and porosity and measurements of electrical conductivity. Different investigation techniques including SEM, TGA, DSC, X-ray, FTIR, particle size distribution and conductivity measurements were used. The electrical conductivity of the composites is $< 10^{-15}$ MS/m, unless the metal content reaches the percolation threshold of 14.4% (v/v), beyond which the conductivity increases markedly by as much as 14 orders of magnitude. It was found that this transition occurs at lower volume fractions than stated in the literature which can be due to the filler with high specific area.

Keywords: Conducting polymer composites, electrolytic copper powder, constant current, lignocellulose, morphology, electrical conductivity, percolation threshold

1. INTRODUCTION

Tailoring new composites within a perspective of sustainable development is applied to more and more materials. Ecological concerns have resulted in a renewed interest in natural, renewable resources -based and compostable materials, and therefore issues such as materials elimination and environmental safety are becoming important. For these reasons, material components such as natural

fibers, biodegradable polymers obtained from biomass can be considered as “interesting” – environmentally safe – alternatives for the development of new biodegradable composites (biocomposites). These polymers show a large range of properties and at present, they can compete with non-biodegradable polymers in different industrial fields (e.g., packaging, agriculture, hygiene, and cutlery) [1]. With their environmentally friendly character and some techno-economical advantages, these natural fibers motivate more and more different industrial sectors such as automotive e.g. to replace common fiberglass [2].

Lignocellulosic biomass is the nonstarch, fibrous part of plant material and is an attractive resource because it is renewable and abundant [3,4]. Lignocellulose-based fibers are the most widely used since, intrinsically, these fibers have a number of interesting mechanical and physical properties [5,6]. The structural and chemical composition of lignocellulosic feedstocks is highly variable because of genetic and environmental influences and their interactions [3]. Chemical composition of lignocellulosic feedstocks is a key factor affecting properties of this biodegradable polymer and its composites [7].

Lignocellulose is the term used to describe the three-dimensional polymeric composites formed by plants as structural material. It consists of variable amounts of cellulose, hemicellulose and lignin [3].

Lignocellulosic feedstocks are composed primarily of carbohydrate polymers (cellulose and hemicellulose) and phenolic polymers (lignin). Lower concentrations of various other compounds, such as proteins, acids, salts and minerals, are also present. Cellulose, the most abundant naturally occurring plant polysaccharide, consists of long chains of anhydro- β -D-glucopyranose units (AGU) with each cellulose molecule having three hydroxyl groups per AGU, with the exception of the terminal ends, whereas hemicellulose is the second most abundant plant polysaccharide readily available, especially from annual plants and agriculture crop residues such as corn cobs, corn grain, wheat stems, seed coats, and sugar cane stalks. Polysaccharides associated with hemicellulose constitute the cell wall of land plants; D-glucuronic acid, L-arabinose, and D-xylose are present in the cell wall of corn cobs in the approximate ratio of 2:7:19, respectively [5]. Lignin (15–25% of total feedstock dry matter) is polyphenolic structural constituent of plants. It is the largest non-carbohydrate fraction of lignocellulose. Other compounds present in lignocellulosic feedstocks are known as extractives. These include resins, fats and fatty acids, phenolics, phytosterols, salts, minerals, and other compounds [5,8].

Both cellulose and hemicelluloses have favorable properties for potential use in the biomedical area, as they have the ability to pass through the digestive tract unchanged. Owing to their resistance to digestion, they are eligible as potential excipients that could be used in the pharmaceutical industry [8].

Biocomposites are obtained by the combination of biodegradable polymer as the matrix material and fillers [2]. The research effort on electrically conducting polymer composites filled with metallic powders has had a great development in the last two decades. The addition of metals fillers into a polymer matrix enables the preservation of the mechanical properties of the polymer while exploiting the electrical conduction properties of the metal [6]. The conductivity of filled polymers is usually strongly dependent on the nature of the contact between the conductive filler elements and

depends critically on the volume fraction of the conducting filler particles, and is well explained by percolation theory [9,10].

Information about numerous existing possibilities of polymers containing dispersed conductive fillers and various methods of manufacture of such materials have been reported widely in the literature for the last years [8,11-22]. Metal-filled conducting polymer composites have found uses in electromagnetic shielding of computers and electronic equipment, as conducting adhesives in electronics packaging, underfill for flip chips, cold solders, switching devices, static charge dissipating materials and devices for surge protection [6,23,24]. Also they found numerous technological applications as self regulating heater, photothermal optical recording, direction finding antennas, chemical detecting sensors used in electronic noses, chemical and electrochemical catalysts and adsorbents [5,12,25-29].

These polymer-based electrically conducting composites have several advantages over their pure metal counterparts, including lower cost, ease of manufacture, high flexibility, reduced weight, mechanical shock absorption ability, corrosion resistance and conductivity control [6].

For efficiency and in order to decrease the difficulty of the process and economic costs, the amount of the conductive phase for achieving materials with high conductivity should be usually as small as possible. The percolation threshold is typically 15–30 vol.% for dense spherical micron size particles [6,12,23,24]. A huge number of different models have been proposed for the estimation of the conductivity (or inverse resistivity) vs. filler concentration curves [30-35].

The electrolytic powder production method usually allows products of high purity which can well be pressed and sintered. Besides, in recent years it has been shown that by different electrolysis regimes it is possible not only to obtain powders with a wide range of properties but to predict the decisive characteristic of powders which are of vital importance for the powder quality and for the appropriate purpose [36,37].

For metal powder application, a series of their properties are of interest; the size and shape of the particles, the bulk weight, flow rate, the corrosion resistance, the specific surface area, the apparent density and the quality of the sintered products. Finally, the properties mentioned depend on the shape and the size of the particles which can be influenced by electrolysis regimes [37-39]. Generally speaking, the larger the powder specific surface the lower its apparent density, and all the more so the smaller the particle size. On the other hand, it seems to be that particle structure has the vital importance on apparent density and on the powder quality.

Since the conductivity of filled polymers is strongly dependent on the nature of the contact between the conductive filler elements, the galvanostatically produced copper powder was chosen in order to enable more contacts between filler's particles.

Copper powder produced in this manner has distinct dendritic morphology and large specific area [37-39], which are preconditions for formation of greater number of contacts with lower volume fraction of the metal fraction in composite.

The aim of this work was to investigate electrical properties of electrolytic copper powder filled lignocellulose matrix composites produced under different pressures, as well to compare the obtained results with previous research in this field and percolation theories.

2. EXPERIMENTAL PART

2.1. Electrolytic copper powder

In order to obtain the most dendritic copper powder, it should be deposited galvanostatically. The experiments were performed in the enlarged laboratory plastic reactor with a cell volume of 10 dm³. Electrolytic copper powder has been produced from electrolyte containing 140 g/dm³ sulfuric acid and 15 g/dm³ copper ions, using an electrolyte temperature (50±2) °C [37,40]. The electrolyte circulation system was designed to supply the laboratory scale cell from one electrolyte supply tank (100 dm³).

The enlarged laboratory reactor had a circulation pump, inlet and outlet for the electrolyte and a heat exchanger. The latter controlled the electrolyte temperature. Electrolyte was pumped from basement storage tank to enlarged laboratory reactor; (electrolyte circulation rate: 0.11 dm³/min). From there, it flowed by gravity and then into the back and the top of the cell. Thus circulation of electrolyte in the tanks was top to bottom. This yields a finer, more homogeneous powder than bottom to top circulation. Electrolyte returns to the basement storage by gravity.

The cell was loaded with four copper cathodes at a spacing of 30 mm between centers [each holding four vertical copper rods (120 mm long, 8 mm diameter)], and five copper anodes (120x120x10)mm which were hung between the cathodes. The distance between anodes was 60 mm from center to center of each anode. The electrodes in the cell were in parallel with each other.

Electrolytic copper powder was deposited galvanostatically at current density of 3600 A/m². The electrolytes were prepared from technical chemicals and demineralized water. The deposition time (time of powder removal by brush) was 15 min.

The wet powder was washed several times with a large amount of demineralized water until the powder was free from traces of acid, at room temperature; the latter promotes rapid oxidation of the powder during drying. It is essential that washing takes place immediately, so that oxidation of the copper particles is precluded. To inhibit oxidation, sodium soap SAP G-30 was added as stabilizer (0.1 wt. %) to water for washing copper powder, to protect the powder against subsequent oxidation [41]. (SAP G-30 contains 78% of total fatty acids). This substance was removed by further washing.

The powder was subsequently dried in tunnel furnaces at 110 – 120 °C in a controlled nitrogen atmosphere.

Particle size distribution of obtained copper powder was analysed using Malvern Instruments laser diffractometer Mastersizer 2000 with the Scirocco 2000 module.

Quantitative microstructural analysis of the copper powder was recorded by Leica Q500 MC (“Reichert-Jung”) [42,43].

The morphology of the deposits was further investigated by means of scanning electron microscopy using a VEGA TS 5130MM microscope (Tescan).

2.2. Lignocellulose

Given that one of the most abundant sources of lignocellulose is corn cob, the matrix natural polymer used in experiments was a commercial grade lignocellulose produced by Maize Research

Institute "Zemun Polje". Celgran[®] C fraction was used [44], milled and then sieved, with particle size below 88 μm .

Thermal stability of the lignocellulose was investigated by thermogravimetry using TA Instruments Q600 thermal analyzer at 10°C/min heating rate under dynamic nitrogen atmosphere. Q100 instrument was used for Differential scanning calorimetry (DSC analysis). Analysis was performed from -50°C to 200°C with 10°C/min heating rate.

Fourier transform infrared spectroscopy (FTIR) was recorded on stabilized copper powder, lignocellulose and lowest and highest copper powder content composites. Michelson MB Series Bomen FTIR was used (Hartmann Braun), scanning from 500 to 4000 cm^{-1} .

X-ray diffraction was carried on lignocellulose matrix. X-Ray Diffractometer XRD 6000 (40kV) from the manufacturer Shimadzu was used. Data were recorded between 0° and 50° 2 Θ , with a step of 0.02°.

Particle size distribution of used lignocellulose was analysed in the same manner as copper powder, using Malvern Instruments laser diffractometer Mastersizer 2000 with the Scirocco 2000 module and morphology of matrix was investigated by means of scanning electron microscopy using a VEGA TS 5130MM microscope (Tescan).

Investigated lignocellulose and copper powder composites were prepared with filler contents in the range 4.3% (v/v) – 42.1% (v/v), while pure lignocellulose and copper samples were prepared as reference materials. The samples were produced from thoroughly homogenized powder mixtures that were pressed into 16 mm diameter tablets at ambient temperature ($t = 25\text{ }^{\circ}\text{C}$) under pressures of 10, 20 and 27 MPa.

Sample thickness (necessary for the calculation of porosity and conductivity) was determined using micrometer, to an accuracy of 0.01 mm. Several thickness measurements were taken per sample and then averaged.

Electrical conductivity measurements were carried out by DC U/I-characteristic measurements of the samples using Digital Multimeter, Model 464, Simpson Electric Company. Geometry of the instrument contacts (rings) used is such that it minimizes edge effects thus it can be assumed that they do not exist.

Hardness of the samples was determined at ambient temperature ($t=25\text{ }^{\circ}\text{C}$) using Shore D hardness testing method in accordance with ASTM D 2240-68 standard. Five data points were taken for each sample and no difference was found between values obtained for both faces of each sample.

3. RESULTS AND DISCUSSION

The method most often employed to alter the electrical properties of a polymer is an extrinsic approach whereby the insulating polymer is combined with a conductive additive. The electrical conductivity of polymer composites does not increase continuously with increasing electroconductive filler content. Hence, in general, the percolation theory is used to describe the nonlinear electrical conductivity of extrinsic conductive polymer composites. The conducting additive is incorporated into polymers at levels that allow the composite to maintain its electrically insulative qualities, as well as at

higher levels, which allow the composite to become electrically semiconductive. As the volume fraction of the conducting filler particles increases, the particles come into contact with one another to form the conduction paths through the composite. As the result there is a critical composition (percolation threshold) at which the conductivity increases by some orders of magnitude from the insulating range to values in the semiconductive or metallic range [9,12,45].

As previously mentioned, the conductivity of filled polymers is strongly dependent on the nature of the contact between the conductive filler elements. Therefore, the copper powder was galvanostatically produced since it should have distinct dendritic morphology and large specific area [37-39].

The apparent density of electrodeposited copper powder was 0.557 g/cm^3 , and the results of quantitative microstructural analysis are shown in Table 1 and Figures 1 and 2. The symbols used have the following meanings:

- A (area) – Feature area (the total number of detected pixels within the feature).
- D_{\max} – Diameter (length) of the largest (longest) particle.
- D_{\min} – Diameter (length) of the smallest (shortest) particle.
- L_p (perimeter) – The total length of the boundary of the feature. This is calculated from the horizontal and vertical projections, with an allowance for the number of corners.
- f_A (form area) – A shape factor of area. This is calculated from the ratio:

$$f_A = \frac{4A}{\pi \cdot D_{\max} \cdot D_{\min}} \quad (1)$$

and for a circle and ellipse is equal to 1.

- f_L (form perimeter) – A shape factor of perimeter. This is calculated from the ratio:

$$f_L = \frac{4\pi A}{L_p^2} \quad (2)$$

and for a circle and ellipse is equal to 1.

- f_R (roundness) – A shape factor which gives a minimum value of unity for a circle. This is calculated from the ratio of perimeter squared to area:

$$f_R = \frac{L_p^2}{4\pi \cdot A \cdot 1.064} \quad (3)$$

The adjustment factor of 1.064 corrects the perimeter for the effect of the corners produced by the digitization of the image.

- f_w – This is the ratio of the length of the polygon circumscribing the feature formed by tangents to its boundary (very similar to the length of a piece of string stretched around the feature) to perimeter.

Table 1. Parameters which characterize sieved fraction ($\leq 88\mu\text{m}$) of electrolytic copper powder deposited galvanostatically at current density of 3600 A/m^2

	Max	Min	Mean
A (area) (μm^2)	1189.52	8.23	198.34
L_p (perimeter) (μm)	368.10	1.91	128.52
D_{max} (μm)	104.71	4.31	55.17
D_{min} (μm)	27.22	0.96	11.42
f_A (form area)	1.00	0.38	0.75
f_L (form perimeter)	0.86	0.13	0.52

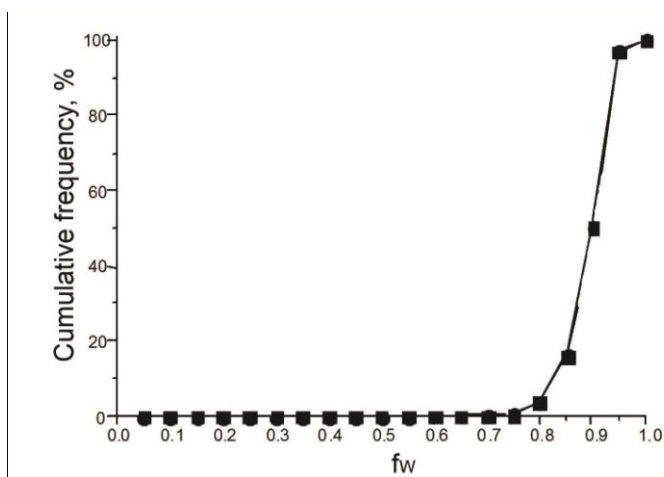


Figure 1. Cumulative frequency as a function of f_w for copper powder

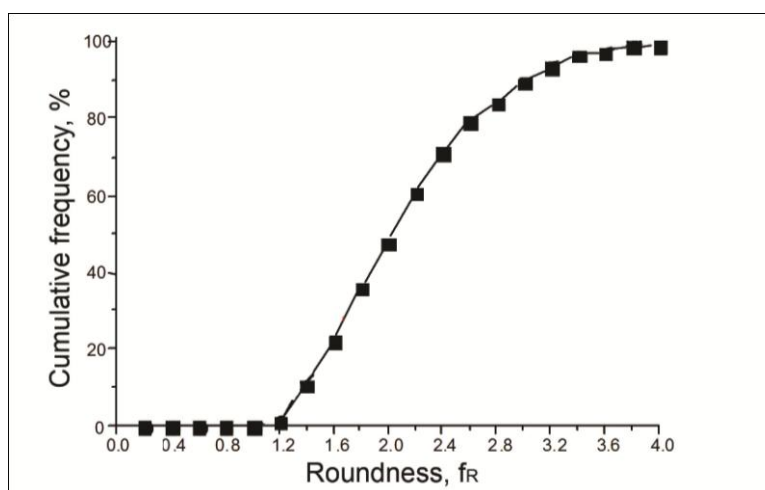


Figure 2. Cumulative frequency as a function of roundness for copper powder

The results of the obtained copper powder show that the powder has very high surface area. f_R or roundness of the particles, which has the smallest values for circle, shows very distinct features for highly dendritic particles with well developed primary and secondary dendrite arms with the angles

between them typical for the face centered cubic crystals. This feature can be seen on Figure 3b, which shows typical copper powder particle obtained by constant current deposition, while Figure 3a shows general view of the powder particles. f_L and L_p values show that copper powder particles are not very compact and rounded, but have pronounced dendrite branching. Hence, this powder is good prerequisite for formation of more interparticle contacts between conductive copper particles and lowering the percolation threshold.

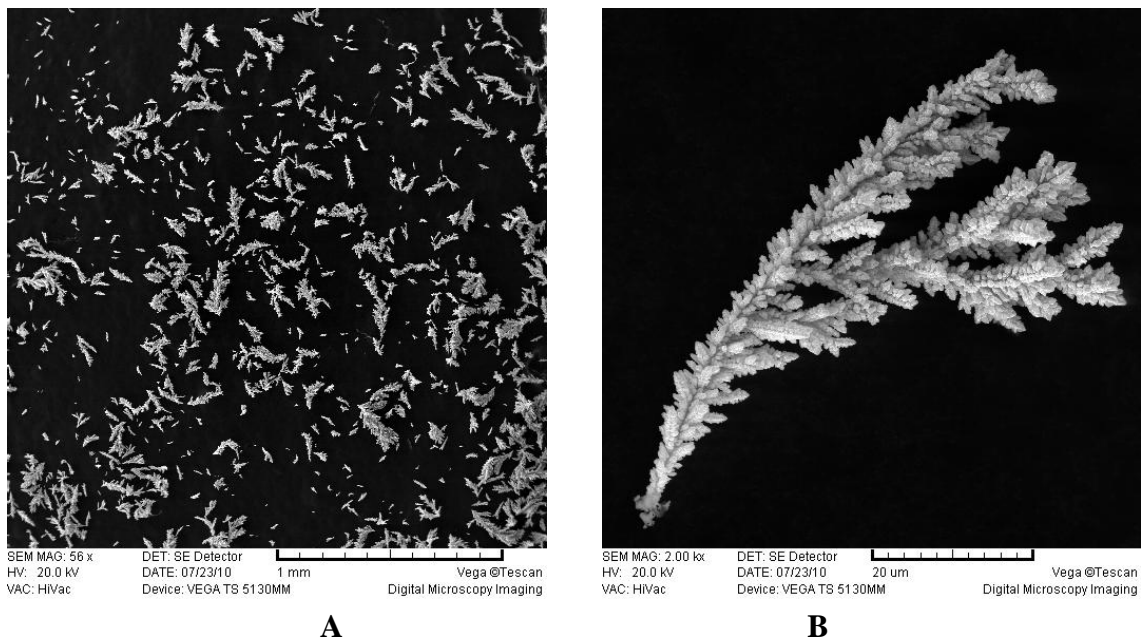


Figure 3. SEM photomicrographs of copper powder particles obtained in constant current deposition. a) general view b) typical powder particle

Particle size distribution curve of produced electrolytic copper powder is presented in Figure 4.

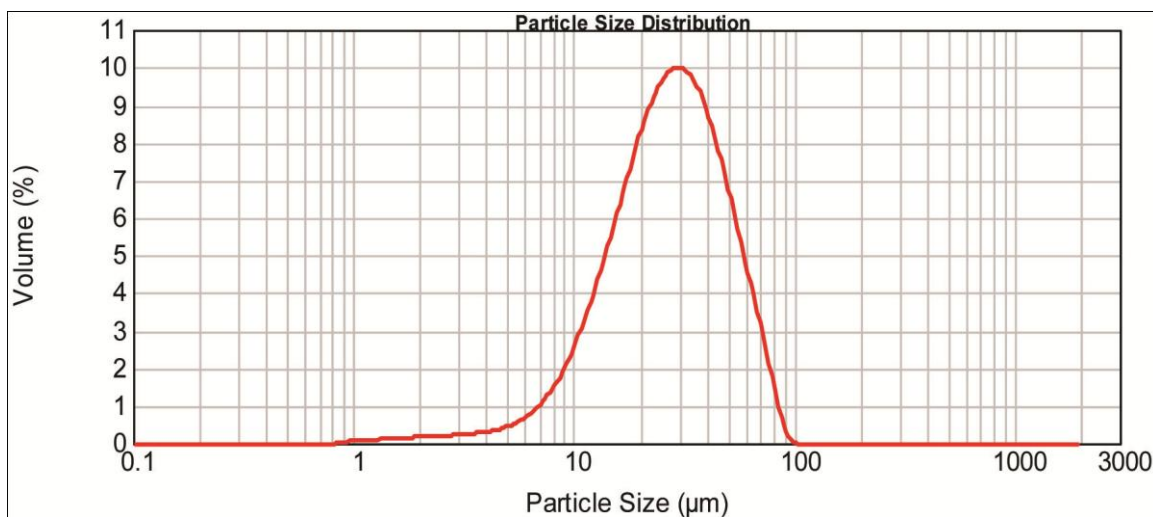


Figure 4. Copper powder particle size distribution curve

The particles show rather uniform size distribution with the mean particle size of copper powder determined by laser diffractometry having following values: $d(0.1) = 11.329 \mu\text{m}$, $d(0.5) = 27.219 \mu\text{m}$ and $d(0.9) = 55.074 \mu\text{m}$.

Figure 5a shows SEM photomicrographs of the used lignocellulose. In Figure 5b distinct layered structure of the lignocellulose bionanocomposite can be observed.

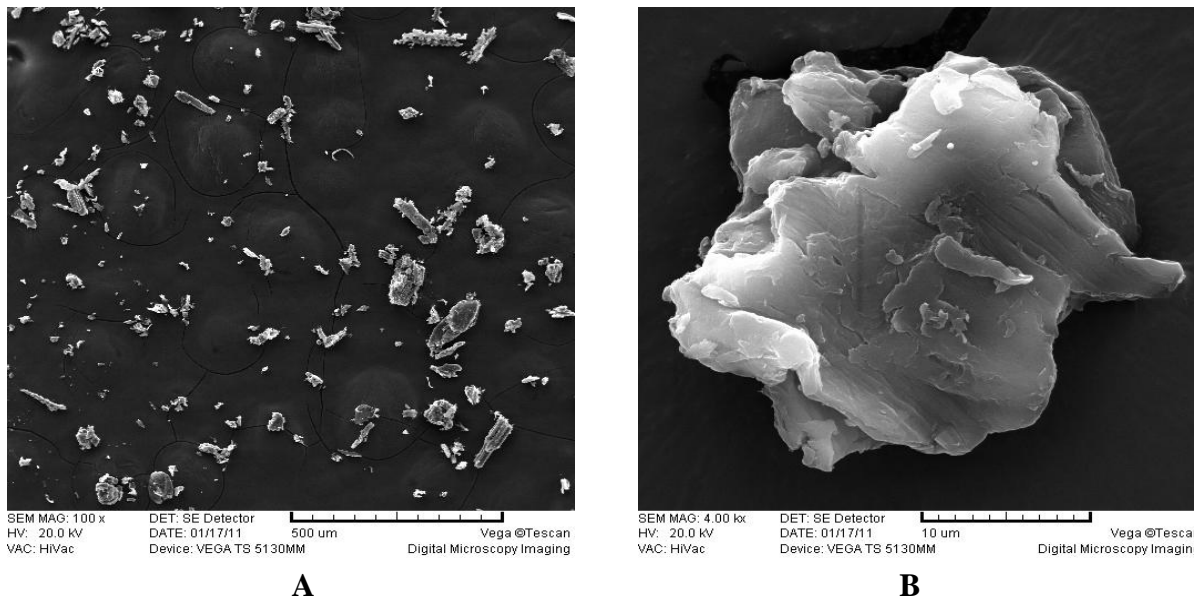


Figure 5. SEM photomicrographs lignocellulose matrix used in composite preparation. a) general view b) typical particle view (layered structure)

Lignocellulose powder used for composite preparation has particle size distribution presented in Figure 6.

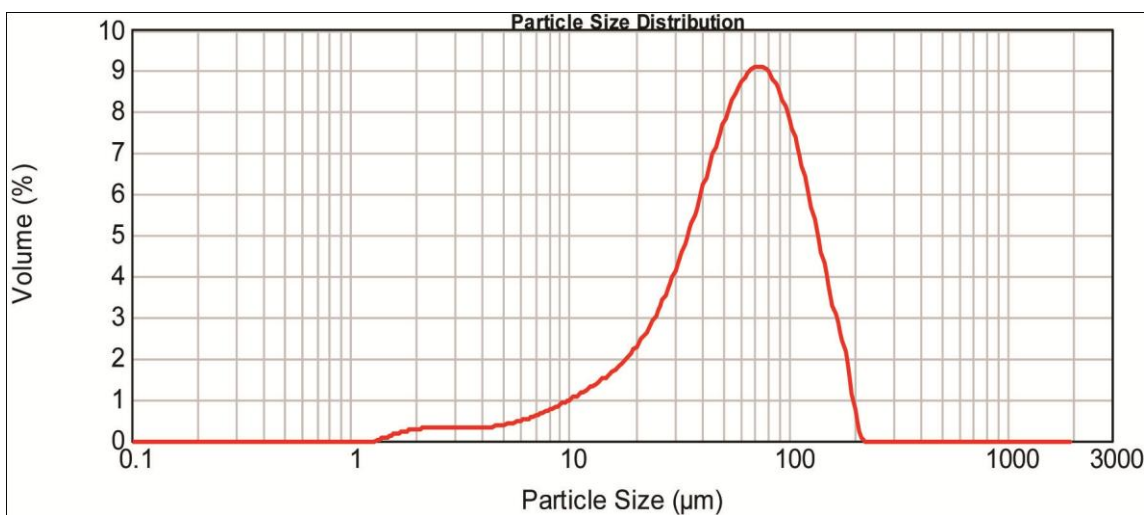


Figure 6. Particle size distribution curve of used lignocellulose matrix

Lignocellulose particles show wider size distribution than the copper powder particles, with less uniformity and with higher volume fractions of larger particles. The mean particle size of lignocellulose powder determined by laser diffractometry has following values: $d(0.1) = 16.833 \mu\text{m}$, $d(0.5) = 60.544 \mu\text{m}$ and $d(0.9) = 127.909 \mu\text{m}$.

Obtained TGA curve, presented on Figure 7, illustrates thermal behavior (stability) of used lignocellulose. Characteristic temperatures of the observed thermal events confirm presence of the main constituents (cellulose, hemicellulose and lignin) [44].

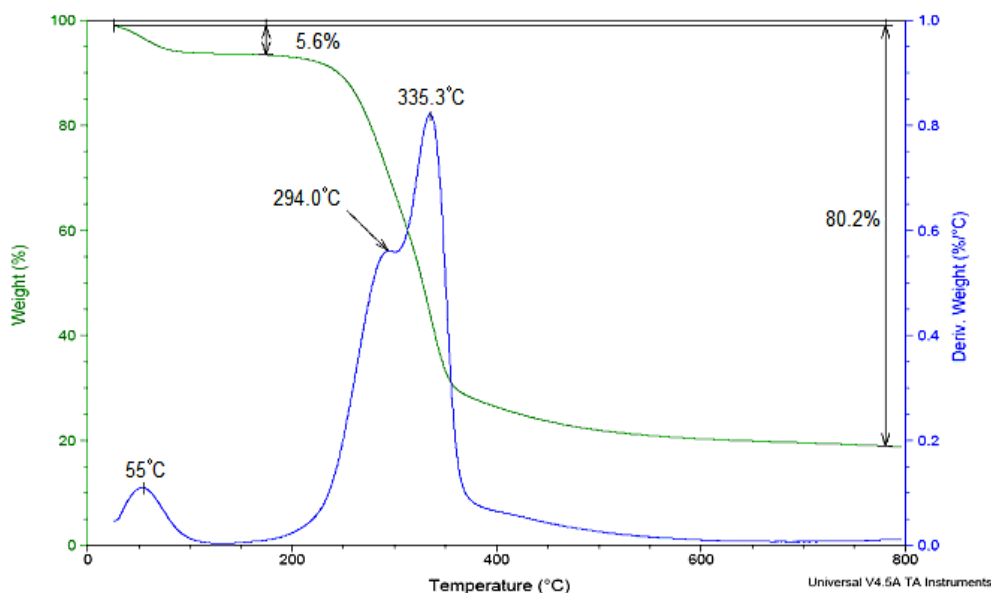


Figure 7. Results of thermogravimetric analysis of lignocellulose - fraction Celgran[®] C

The mass loss increases with temperature gradually up to approximately 200 °C, while in the region between 200 and 400 °C more significant mass loss occurs. On the obtained TGA curve (Figure 7) two distinct peaks can be observed within this temperature interval, suggesting the existence of two separate thermal events. According to the literature data [46-48], the first event that occurs at 210-300 °C can be associated with the decomposition of hemicellulose and the slow degradation of lignin, while the second event (275-350 °C) can be attributed to the degradation of cellulose. Possible discrepancies between literature data and the TGA results may be associated with the amount of cellulose and lignin in the lignocellulose material, given that Shebani et al. [46] and D'Almeida et al. [49] demonstrated that higher cellulose and lignin content in lignocellulosic materials leads to a greater thermal stability.

Smaller peak at 55°C on TGA curve can be associated with the endothermic event (55.8°C) observed at DSC curve of used lignocellulose fraction Celgran[®] C, presented in Figure 8. This event most probably corresponds to glass transition temperature of hemicelluloses or lignin given that according to Furuta et al. [50] the glass transition temperature for hemicelluloses is around 40 °C and about 50 °C to 100 °C for lignin. Many authors have reported the glass transition of wood and its chemical components under various conditions and they differ considerably, especially considering

that the decrease of the moisture content of wood increases the glass transition temperature [51]. In general, for green wood lignin, the glass transition is around 60 °C [52].

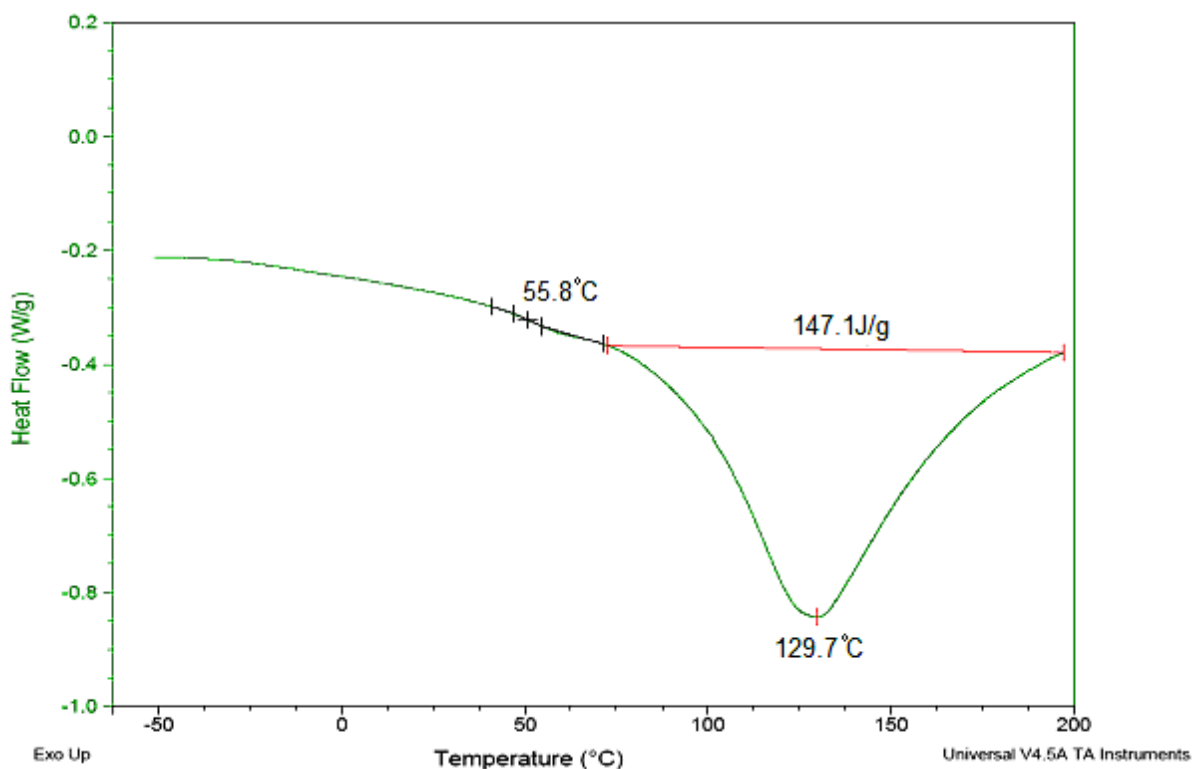


Figure 8. DSC curve of used lignocellulose fraction Celgran[®] C

On the presented curve (Figure 8) more prominent endothermic event can be observed in the temperature interval 70°C to 200°C with the peak around 129.7 °C. In accordance with [53] it can be assumed that this event is related to release of water associated with hydration of lignocellulosic structure, before macromoleclar chain degradation occurred.

XRD results (Figure 9) show that the diffraction pattern of lignocellulose – fraction Celgran[®] C is consistent with the structure of cellulose I [54,55]. Peaks corresponding to crystallographic planes 101 (14.7), $10\bar{1}$ (16.24), 021 (21.15) and amorphous (17.64) characteristic to cellulose I can be observed.

Figure 10 shows results of the FTIR spectra of the measurements performed on stabilized copper powder, lignocellulose and 4.2% (v/v) and 42.1% (v/v) copper powder content composites. FTIR spectrum of the Cu powder shows three distinct peaks: at 3423.0 cm⁻¹ characteristic for O-H alcohol groups, at 2921.9 cm⁻¹ characteristic for C-H methyl and methylene groups and at 1623.2 cm⁻¹ characteristic for C=C alkene bonds.

This is in good agreement with statement that copper powder was stabilized with sodium soap SAP G-30, which contains 78% of total fatty acids, in order to protect the powder against subsequent oxidation.

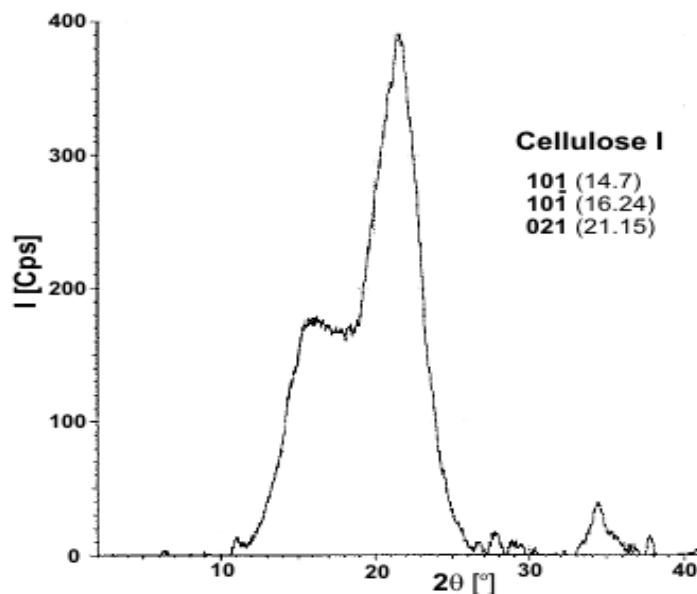


Figure 9. X-ray diffraction pattern of the lignocellulose fraction Celgran® C

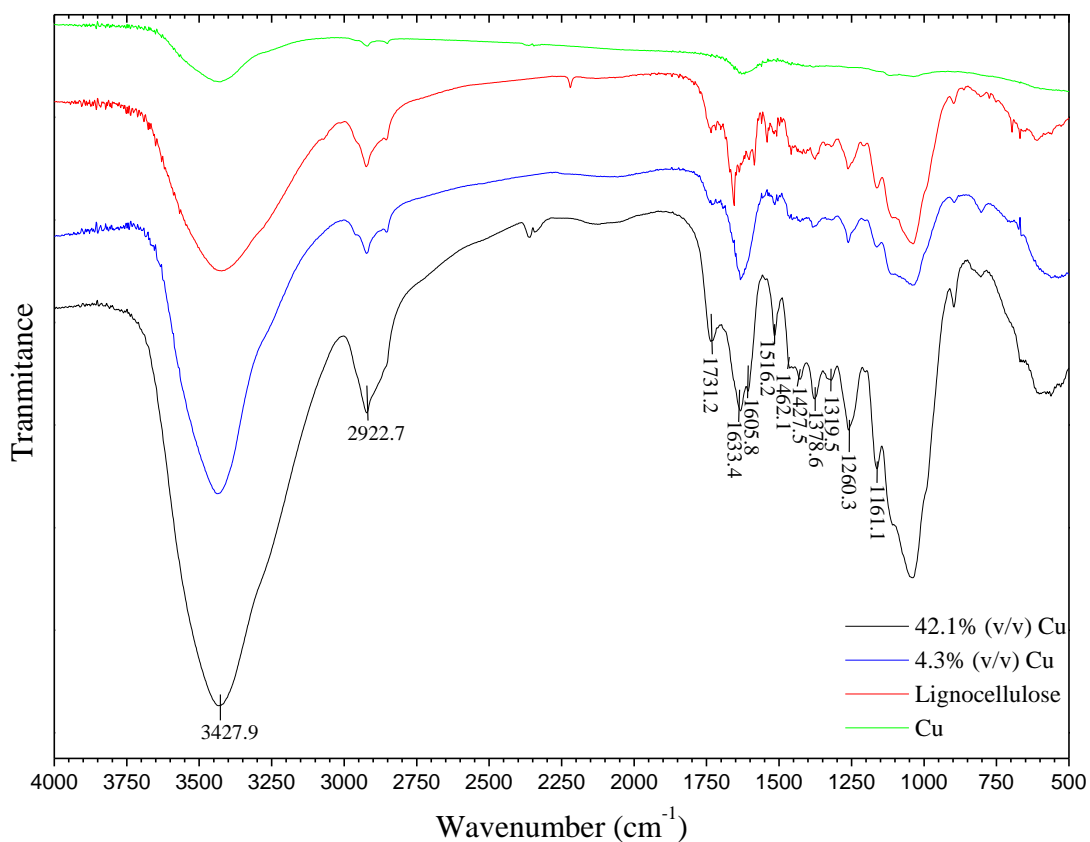


Figure 10. FTIR spectra of the pure stabilized copper powder, lignocellulose and their composites

Other characteristic FTIR band positions for the lignocellulose and copper filled lignocellulose composites are given in Table 2.

Table 2. Assignment of the IR bands of functional groups

Band position (cm ⁻¹)	Functional group
3423.7	O-H alcohol
2922.7	C-H methyl and methylene groups
1731.2	C=O carbonyls
1633.4, 1605.8	C=C alkene (absorbed water and β-glucosidic linkages between sugar units)
1516.2	C=C aromatic
1462.1, 1427.5	CH ₂ cellulose, lignin
1378.6, 1319.5	C-H cellulose (crystallized and amorphous), hemicellulose
1260.3	O-H phenolic
1161.1	O-H alcohols (primary and secondary) and aliphatic ethers

It can be concluded that there is no chemical reaction occurring between lignocellulose and copper powder, and that the influence of the O-H, C-H and C=C groups on the spectra is amplified as the copper powder content increases in the composite. There is slight or no shift in the wavenumber between the studied samples.

Theoretical density of composites, ρ_t , was calculated according to relation [12,56]:

$$\rho_t = (1 - V_f)\rho_m + V_f\rho_f \quad (4)$$

where V is volume fraction, ρ – density while f and m indexes correspond to filler (copper powder) and matrix (lignocellulose), respectively.

Porosity of the investigated composites, τ , was determined by comparison of experimental and theoretical densities of the samples according to relation [12,56]:

$$\tau = \left(\frac{\rho_t - \rho_e}{\rho_t} \right) \times 100 \quad (5)$$

where ρ_e – is experimentally obtained value of composite density.

Electrical conductivity was determined according to relation:

$$\sigma = \frac{I}{U} \cdot \frac{l}{S} \quad (6)$$

where σ is electrical conductivity, I – current through sample, U – potential difference, l – length and S – cross-section area of the sample.

Figure 11 represents the porosity rate of different composites as function of the filler volume fraction at various processing pressures. It can be seen that, as expected, the porosity decreases with the increase of pressure, due to higher packaging effect. On the other hand, as the volume fraction of

the very porous natural matrix decreases, the porosity decreases as well. In all cases, the porosity is still rather high around percolation threshold and it is between 24% and 30%. These results show that although the quality of the obtained composites was good, some changes in the preparation processes can lead to lower porosity composites.

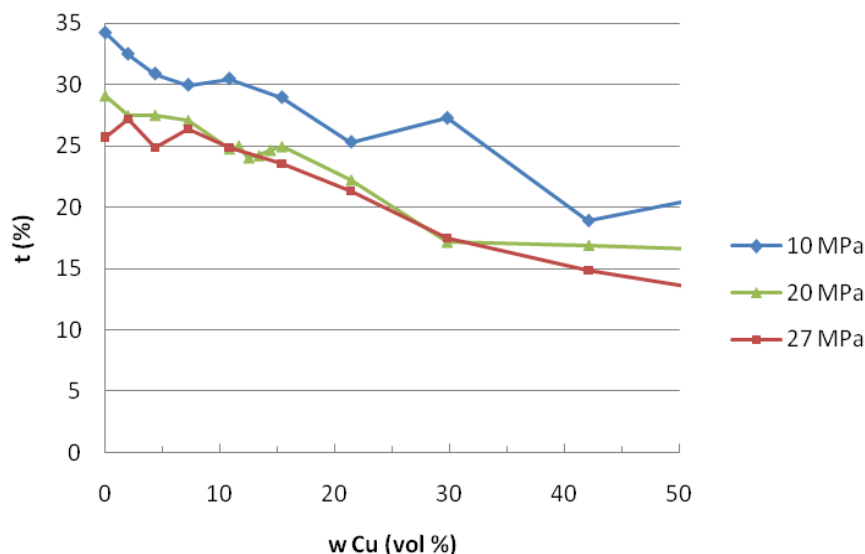


Figure 11. Porosity of the copper powder filled lignocellulose matrix composites at various pressures

Figure 12 shows the dependence of hardness measured as shore D values, in various composites of lignocelluloses matrix and copper powder filler prepared under various pressures. Hardness of the investigated composites, as expected, increases with the increase of the molding pressure. However, it is obvious that increase of the filler fraction has less significant influence on the hardness values, resulting in approximately constant values, nearly independent of the filler fraction.

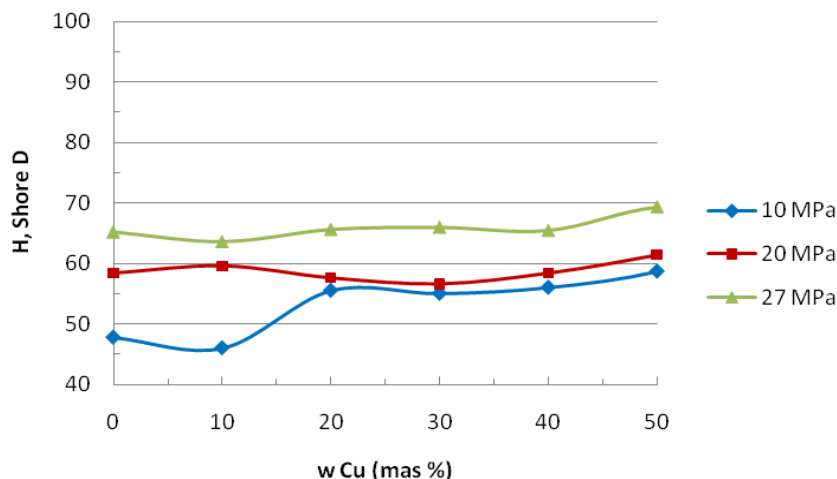


Figure 12. Hardness of lignocelluloses matrix and copper powder filler composites prepared under various pressures. Measurements are shown as Shore D values

The electrical conductivity of the composites as a function of filler content for all the samples was measured as stated in Experimental part. The conductivity measurements (Figure 13) showed typical S-shaped dependency with three distinct regions: dielectric, transition and conductive.

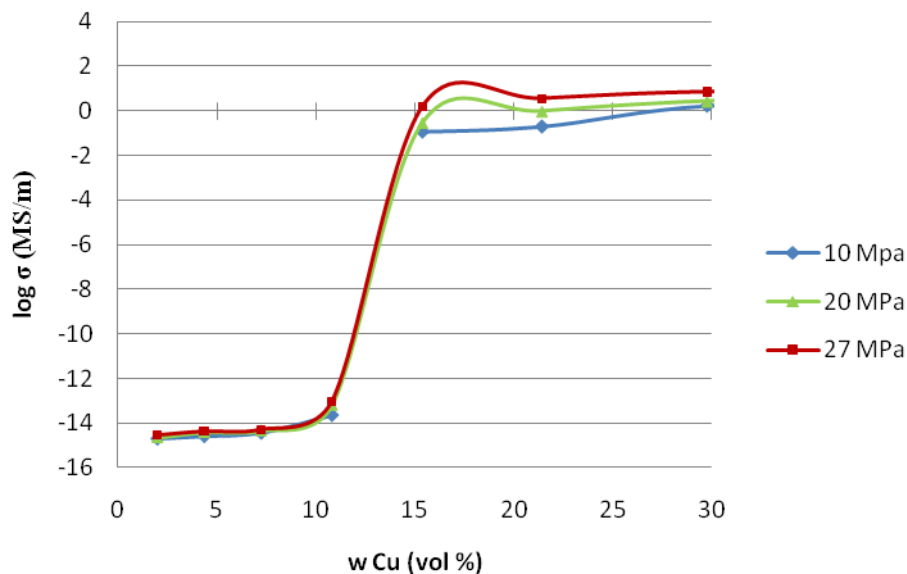


Figure 13. Variation of electrical conductivity, as a function of filler content, of lignocellulose composites filled with copper powder under different processing pressures

Clearly, the samples with low filler content are practically nonconductive. Naturally, the electrical conductivity of the composites increases with the increase of the conductive filler content. The significant increase of the electrical conductivity can be observed as the copper content reaches the percolation threshold at 14.4% (v/v) for all the processing pressures. The value of the percolation threshold was obtained from the maximum of the derivative of the conductivity as a function of filler volume fraction (Figure 13). Obtained values of percolation threshold are lower than those stated in previous study by Flandin et al.[16], which shows that for spherical particles of the filler values of 20–40% (v/v) are typical. This much lower percolation threshold can be explained by much higher specific area of the highly dendritic electrolytic copper powder particles used as filler. According to the statistical percolation theory [33,34], which is usually used to explain the electrical conductivity of the composites, the existence of clusters of connected particles gives the rise to the so-called conducting infinite cluster above the threshold. With highly porous, highly dendritic particles with high values of specific area, more interparticle connections can be obtained at lower filler content. It can be seen from Figure 13 that under investigated range of pressures there is no change in the percolation threshold. More precise measurements should be made around percolation threshold in order to determine possible small change in the threshold point. However, in the conductive region, composites with the same volume fraction of copper powder prepared under higher pressure have higher values of conductivity. Above the percolation threshold, the conductivity of composite increased by much as fourteen orders of magnitude. The increase in the conductivity is higher than

stated by Pinto et al. [12] which can be contributed to use of electrodeposited copper powder filler with high specific area.

4. CONCLUSIONS

In this article, experimental study about the effects of electrodeposited copper powder content on the electrical conductivity of composites of lignocellulose matrix filled with powder of that metal has been described. Results have shown that the powder has very high surface area and it has pronounced dendrite branching with well developed primary and secondary dendrite arms. The conductivity measurements showed S-shaped dependency with percolation transition from non-conductive to conductive region, typical for such polymer composite materials. For a given range of filler concentration and pressures the increase of the electrical conductivity of composites is as much as 14 orders of magnitude, and it is higher than stated by Pinto et al. [12] with the same filler and similar matrix. This increase can be attributed to high specific area of used copper powder. The percolation threshold concentration corresponds to a volume fraction of copper of 14.4% (v/v) and it is in good agreement with percolation theory and the experiments that can be found in literature. Given that the porosity results show that increase in the processing pressure leads to smaller porosity, and considering that the lignocellulose is highly porously packed, there is room for improvement in future investigations. The same is eligible for the Shore D hardness.

This research has undoubtedly shown that galvanostatically obtained copper powder plays significant role with its indented area in formation of greater number of contacts with smaller volume fractions. In this manner the value of percolation threshold is lowered. Surely it would be interesting to investigate identical system, but with copper powder obtained at a periodically changing rate in further investigations, as well as, with other electrochemically obtained metal powders.

ACKNOWLEDGEMENT

This work was financially supported by Ministry of Science of the Republic of Serbia under the research projects: ON172046 and ON172037.

References

1. D.K. Lee, V.N. Owens, A. Boe and P. Jeranyama, Composition of Herbaceous Biomass Feedstocks, South Dakota State University (2007)
2. L. Averous and F. Le Digabel, *Carbohydrate Polymers*, 66 (4) (2006) 480
3. S. Jovanović, Ž. Stojanović and K. Jeremić, *Hem. Ind.*, 56 (11) (2002) 447
4. S. Jovanović, G. Nestorović and K. Jeremić, *Hem. Ind.*, 57 (11) (2003) 511
5. M. Ioelovich, *BioResources*; 3 (4) (2008) 1403
6. V.H. Poblete, M.P. A´lvarez and V.M. Fuenzalida, *Polymer Composites*, 30 (2009) 328
7. C.N. Hamelinck, G.V. Hooijdonk, and A.P. Faaij, *Biomass and Bioenergy*, 28 (2005) 384
8. S. Kamel, *Express Polymer Letters*, 1 (2007) 546
9. D.S. McLachlan, M. Blaszkiewicz and R.E. Newnham, *J. Am. Ceram. Soc.*, 73 (8) (1990) 2187

10. L.J. Huijbregts, Charge transport and morphology in nanofillers and polymer nanocomposites, Ph.D. Thesis, Technische Universiteit Eindhoven (2008)
11. V. Bojanić, *Hem. ind.* 64 (6) (2010) 529
12. G. Pinto, A.K. Maaroufi, R. Benavente and J.M. Perena, *Polym. Compos.*, 32 (2011) 193
13. M. Thakur, *Macromolecules*, 21 (1988) 661
14. H.S. Son, H.J. Lee, Y.J. Park and J.H. Kim, *Polym.Int.*, 46 (1998) 308
15. J. Bouchet, C. Carrot and J. Guillet, *J. Polym. Eng. Sci.*, 40 (2000) 36
16. L. Flandin, A. Chang, S. Nazarenko, A. Hiltner and E.J. Baer, *J. Appl. Polymer. Sci.*, 76 (2000) 894
17. E.A. Stefanescu, C. Daranga and C. Stefanescu, *Materials*, 2 (2009) 2095
18. C. Singh, V. Sharma, P. Kr Naik, V. Khandelwal and H. Singh, *Digest Journal of Nanomaterials and Biostructures*, 6 (2) (2011) 535
19. S. Nenkova, P. Velev, M. Dragnevskaja, D. Nikolova and K. Dimitrov, *Bioresources*, 6 (3) (2011) 2356
20. M. A. Cohen Stuart et al., *Nature Materials*, 9 (2010) 101
21. B.A. Rozenberg and R. Tenne, *Prog. Polym. Sci.*, 33 (2008) 40
22. L. Pan, H. Qiu, Ch. Dou, Y. Li, L. Pu, J. Xu and Y. Shi, *Int. J. Mol. Sci.*, 11 (2010) 2636
23. L. Xiangcheng and D.D.L. Chung, *Composites Part B: Eng.*, 30 (1999) 227
24. M.L. Sham and J.K. Kim, *Composites Part A: Appl. Sci. Manuf.*, 35 (2004) 537
25. J. Delmonte, *Metal/Polymer Composites*, Van Nostrand Reinhold, New York (1990)
26. P. Lafuente, A. Fontecha, J.M. Diaz and A.E. Munoz, *Rev. Plast. Mod.*, 447 (1993) 257
27. V.E. Gul, *Structure and Properties of Conducting Polymer Composites*, VSP: New York (1996)
28. B.C. Munoz, G. Steinthal and S. Sunshine, *Sens. Rev.*, 19 (1999) 300
29. J.B. Patel and P. Sudhakar, *EJEAFChe*, 7 (14) (2008) 2735
30. S. Kirkpatrick, *Rev. Mod. Phys.*, 45 (1973) 574
31. F. Lux, *J. Mater. Sci.*, 28 (1993) 285
32. X.B. Chen, J. Devaux, J.P. Issi and D. Billaud, *Polym. Eng. Sci.*, 35 (1995) 637
33. E.P. Mamunya, V.V. Davidenko and E.V. Lebedev, *Compos. Interfaces*, 4 (1997) 169
34. E.P. Mamunya, V.V. Davidenko and E.V. Lebedev, *Polym. Compos.*, 16 (1995) 319
35. S. De Bondt, L. Froyen and A. Deruyttere, *J. Mater. Sci.*, 27 (1995) 319
36. R.M. German, *Powder Metallurgy Science*, 2nd ed., Metal Powder Industries Federation, Princeton, New Jersey, 1994, pp.15–42
37. K.I. Popov and M.G. Pavlović, in *Modern Aspects of Electrochemistry*, Electrodeposition of metal powders with controlled particle grain size and morphology, B.E. Conway, J.O'M. Bockris and R.E. White, Eds., Vol. 24, Plenum, New York, 1993, pp.299–391; M.G. Pavlović, N.D. Nikolić and Lj.J. Pavlović, “The development, improvement and definition of electrochemical technology of copper powder production”, *Copper Smeltery and Refinery, Bor* (2000), (in Serbian)
38. M.G. Pavlović, K.I. Popov and E.R. Stojilković, *Bulletin of Electrochemistry*, 14 (1998) 211
39. M.G. Pavlović, Lj.J. Pavlović, V.M. Maksimović, N.D. Nikolić and K.I. Popov, *Int. J. Electrochem. Sci.*, 5 (2010) 1862
40. M.G. Pavlović, Lj.J. Pavlović, E.R. Ivanović, V. Radmilović and K.I. Popov, *J. Serb. Chem. Soc.*, 66 (2001) 923
41. M.G. Pavlović, Lj.J. Pavlović, I.D. Doroslovački and N.D. Nikolić, *Hydrometallurgy*, 73 (2004) 155
42. R.T. De Hoff, F. N. Rhines, *Quantitative Microscopy*, Mac Graw Hill Book Comp., New York, 1968, p.93
43. H. Modin, S. Modin, *Metallurgical Microscopy*, Butterworths, London, 1973, p.143
44. I. Božović, M. Radosavljević, R. Jovanović, S. Žilić, V. Bekrić and D. Terzić, *J. Sci. Agric. Research*, 63 (3-4) (2002) 37
45. D. Stauffer and A. Aharony, *Introduction to percolation theory*, 2nd ed., Taylor and Francis, London (1992)

46. A.N. Shebani, A.J. van Reenen and M. Meincken, *Thermochimica Acta*, 471 (2008) 43
47. F. Yao, Q. Wu, Y. Lei, W. Guo and Y. Xu, *Polymer Degradation and Stability*, 93 (2008) 90
48. H.S. Kim, S. Kim, H.J. Kim and H.S. Yang, *Thermochimica Acta*, 451(1) (2006) 181
49. A.L.F.S. D'Almeida , D.W. Barreto, V. Calado and J.R.M. D'Almeida JRM, *Journal of Thermal Analysis and Calorimetry*, 91(2) (2008) 405
50. Y. Furuta, H. Aizawa, H. Yano, M. Norimoto, *Mokuzai Gakkaishi* 43(9) (1997) 725
51. C.A. Lenth, F.A.Kamke, *Wood Fiber Sci.* 33(3) (2001) 492.
52. T. Nakano, *J. Wood Sci.* 52 (6) (2006) 490
53. S.N. Monteiro, R.J.S. Rodriguez, L.L. da Costa, T.G.R. Portela, N.S.S. Santos, *Revista Matéria* 15 (2) (2010) 104
54. R.Y. Chen, K.A. Jakes, D.W. Foreman, *J. Appl. Polym. Sci.* 93 (2004) 2019
55. S. Bates, G. Zografis, D. Engers, K. Morris, K. Crowley, A. Newman, *Pharm. Res.* 23 (2006) 2333
56. A.Maaroufi, K. Haboubi, A. El Amarti and F.Carmona, *J.Mater.Sci.* 39 (2004) 265.